Single Cell Detection Capability of an Optofluidic Spectroscopic Biosensor

H. Shao, D. Kumar, and K. L. Lear
Electrical and Computer Engineering Department
Colorado State University
Fort Collins, United States
lshao@engr.colostate.edu

***Abstract*— Biological cells inside an optofluidic cavity modify the optical cavity modes, providing a probe for optical properties of the cells that can be used to detect and differentiate single cells. Transmission spectra of single biological cells including yeast cells and human blood cells as well as polystyrene spheres in a microfluidic Fabry-Perot cavity fabricated on glass substrates are measured and exhibit cell-type specific features attributed to higher order transverse modes. A method for spectral correlation is also presented to verify the preliminary results of the single cell spectra. The correlation calculation demonstrates that the method is able to differentiate some types of single cells.**

I. INTRODUCTION

Rapid detection of single biological cells is of broad interest in a variety of fields, including biology, chemistry, food safety, environmental monitoring, and homeland security. Techniques ranging from direct imaging methods, such as autofluorescence [1] and confocal microscopy [2], to spectroscopic methods, such as confocal Raman [3] and cavity ring-down spectroscopy [4] have been used to detect single biological cells. It is known that optical properties of biological cells can provide substantial information about cell parameters including size, shape, and refractive index variation. Biological cells inside an optofluidic cavity modify the optical cavity modes, providing a probe for optical properties of the cells that can be used to detect and differentiate single cells [5].

This work combines microfluidic and optical sensing techniques to realize real time, label-free detection of single biological cells. The detection and differentiation of cells is based on the transmission mode spectra of cells in 10 to 25μm deep microfluidic Fabry-Perot (FP) cavities fabricated on glass substrates and illuminated by an LED (Hamamatsu L2690-02) with a full width at half maximum (FWHM) of ~30nm as schematically illustrated in Fig. 1. The transmission spectrum of the fluidic cavity was then analyzed with a 0.3 nm resolution Ocean Optic spectrometer (HR2000). Section II discusses the fabrication of the sensor. The transverse mode spectrum of the cell-loaded cavity is determined by the refractive index structure of the cell including its size and shape. Experimental single cell spectra obtained using this method are presented in Section III and qualitatively appear to have characteristics such as the number of modes and mode spacing that can be used to differentiate cells. To further evaluate the utility of this sensor, a method for quantitative calculation of the spectral correlation was developed and evaluated as discussed in Section IV. The results have demonstrated the feasibility of using the biosensors developed in this work to detect certain types of single biological cells.

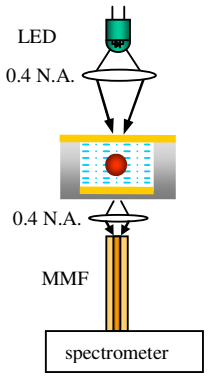

Figure 1. Experimental setup for single cell spectroscopy.

II. DEVICE FABRICATION

Glass-based microfluidic devices are very attractive for microcavity spectroscopy because of their good surface rigidity and smoothness that are favorable for making a high finesse optical cavity. A process based on thermocompressive gold bonding of glass with etched channels has been developed to fabricate microfluidic FP cavities [6]. The cavity was formed by etching 10~25 μm deep and 100~200 μm wide channels in Pyrex glass and coating the surfaces with reflective thin gold layers as the reflectors of the FP cavity. Through holes of 1 mm diameter

0-7803-9056-3/05/$20.00 © 2005 IEEE.

were drilled at the end of the channel before bonding the glass superstrate and substrate in order to incorporate nanoports onto the sensor chip to overcome the capillary force induced fluid flow by pressure balancing using syringes at the end ports of the channel. Fig. 2 shows a SEM cross-section of a 7 µm deep cavity after the thermocompressive wafer bonding and the optical transmission spectra of a ~25 µm deep cavity. The measured cavity finesse, ~30, is in good agreement with the calculations based on the combined effects of the mirror reflectivity, roughness and tilt. Detailed characterization of the device fabrication can be found in reference [6].

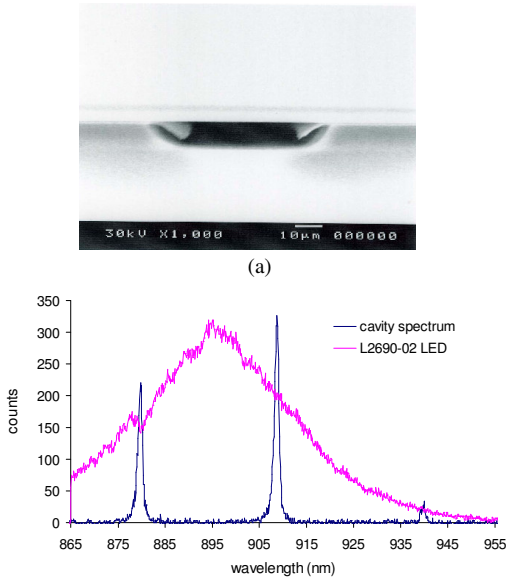

Figure 2. (a) SEM picture of a cavity cross-section after thermocompressive bonding. (b) Microfluidic FP cavity transmission spectrum illuminated with a well-collimated Hamamatsu LED biased with a 100 mA current source.

III. INTRACAVITY SPECTROSCOPY

Spectra of different types of polystyrene spheres and biological cells were measured by introducing them into the fluid filled, etched channels. A biconcave lens (f=30mm) focused the LED light from the bottom to effectively excite the higher order transverse modes of the fluidic cavity. Transmitted light was collected by a multimode optical fiber (62.5µm core diameter) through the customized microscope. The focal length of the optical system was adjusted to make the light collection spot size, i.e. the image size of the light collecting fiber's core, approximately 5 to 10 µm in diameter in order to probe single cells inside the fluidic cavity.

A. Transmission Spectra of Standard Particles

Initial transmission spectra were obtained from the microfluidic cavity filled with a water suspension of polystyrene (n=1.59) and Silica (n=1.45) microspheres (purchased from Bangs Laboratories, Inc.) as they resembled cells but with well controlled size, shape, and index of refraction. Typical transmission spectra for a 5 µm diameter polystyrene sphere and 5.06µm diameter silica sphere together with the illumination conditions are presented in Fig. 3.

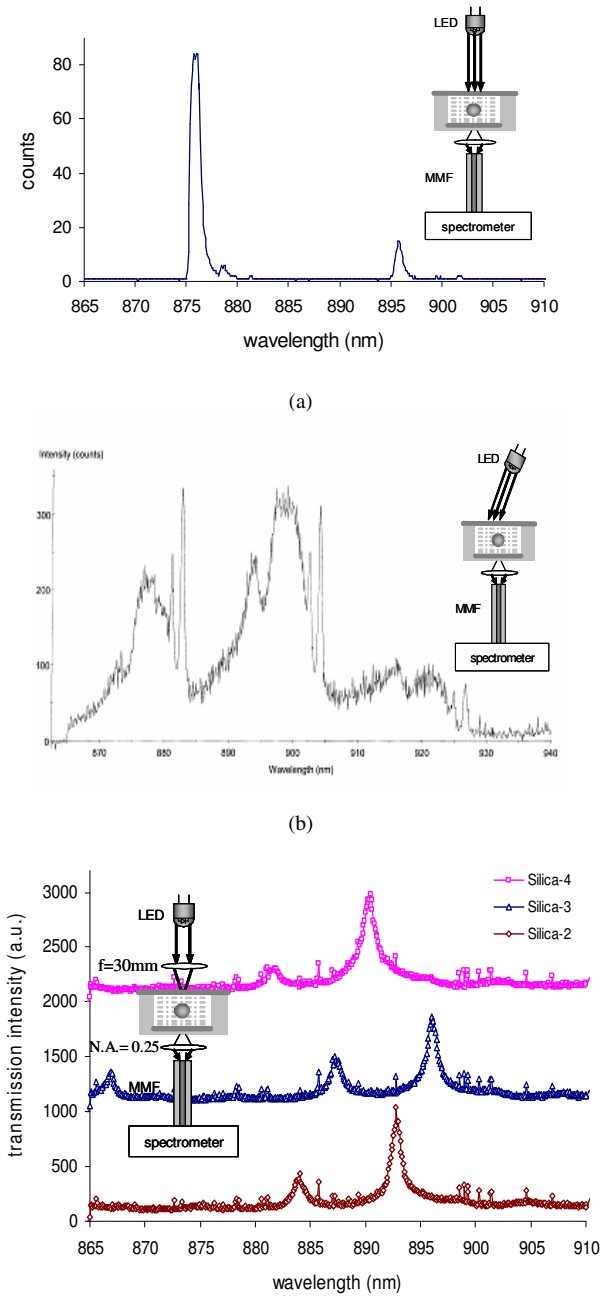

Figure 3. Transmission spectrum of a single 5 µm diameter polystyrene sphere with uniform refractive index of 1.59 submerged in deionized water under (a) normal and (b) tilted illumination in a ~12µm deep fluidic caivty, and (c) tranmssion spectra of three separate single silica microsphere with uniform refractive index of 1.45 in a ~7µm deep fluidic cavity.

The spectrum in Fig. 3 (b) clearly shows additional narrow transmission resonances, corresponding to the transverse cavity modes, compared to the bare cavity modes seen in Fig. 3 (a). The cavity's transverse mode groups are repeated three times, corresponding to three longitudinal modes, within the wavelength range of the LED. The free spectral range of the 12 µm and 7µm deep cavity is ~20 nm and 30nm respectively as shown in Figure 2 (a) and (c). The number of the transverse modes and the spectral differences of neighboring modes provide useful information about the sphere inside the microfluidic cavity [7]. High order transverse modes are effectively excited by the titled illumination as seen in Fig. 3 (b) and (c) because of their relatively larger diffraction angles than the fundamental modes.

B. Transmission Spectra of Single Biological Cells

In the case of real biological cells, the situation is more complicated because of the unknown refractive index, absorption, and nonuniformity of cell geometry. The first biological cell type investigated was yeast cells because of their ready availability and size (8 to 15 µm diameter) compatability with the sensor. Transmission spectra for three separate single yeast cells prepared in water are shown in Fig. 4 and appear relatively similar. The bare cavity mode observed in regions away from the yeast cells is also shown with the dashed line. A shift in wavelength is anticipated between the bare cavity mode and even the fundamental optical mode in the presence of a cell both because of a variation in the transverse optical confinement as well as the integrated optical path length changing due to the cell's higher index of refraction compared to the water. Bare cavity regions or specific cells can be interrogated by simply horizontally translating the fiber optic to accept the image of that region. The relative fiber optic position can be determined by backward illuminating the fiber and observing the light spot relative to the cell positions in the microscope.

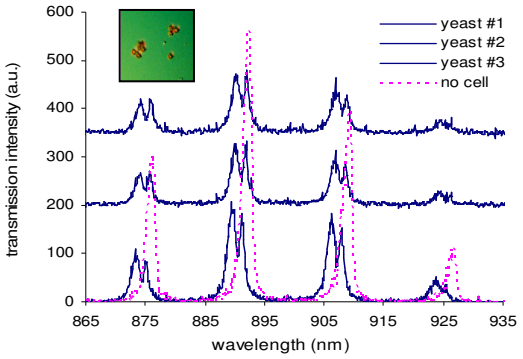

Figure 4. Transmission spectra of three separate single yeast cells. The bare cavity mode spectrum is also shown with the dashed line. The inserted image of the yeast cells was taken by a dark field microscope. The mode exciation condition is the same as shown in Fig. 3 (c).

Next, microfludic FP cavity transmission spectra for several blood cells were obtained. The cells were obtained from a single human body and introduced into the microfluidic cavity without any dilution of the original blood serum. Two distinct types of spectra were obtained corresponding to red blood cells seen in Fig. 5 (a) and what are believed to be various types of white blood cells seen in Fig. 5 (b). The spectral signatures of the different cell types are considered to be sufficiently qualitatively unique to differentiate them. The yeast cells showed a single, relatively broad transmission peak at slightly longer wavelength than what is assumed to be the fundamental mode. The blood cells showed strong, narrow transmission peaks, one for red blood cells and two for white blood cells, at larger wavelength offsets. The amount of offset varies somewhat from cell to cell and may be associated with cell size. Further quantitative cross-correlation analysis of the cell spectra will be presented in Section IV.

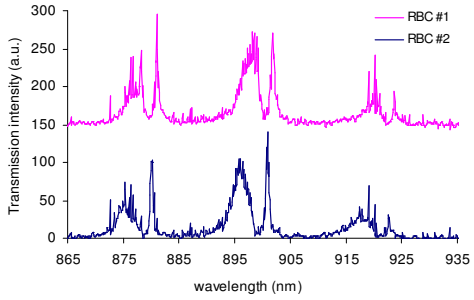

(a)

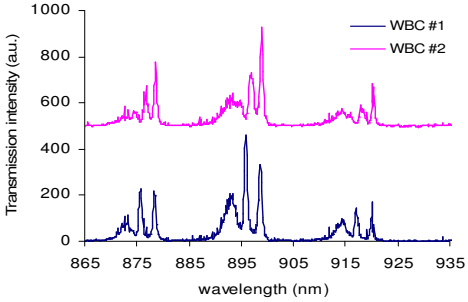

(b)

Figure 5. Transmission spectra of (a) red and (b) white human blood cells. The mode excitation condition is the same as shown in Fig. 3 (c).

Different biological cell's spectra exhibited variations in peak amplitude, mode spacing, and number of higher order transverse modes. All of these spectral differences are attributed to the optical confinement perturbation inside the micro-fluidic FP cavity. Theoretical modeling of the modal structures of the cell loaded microfluidic using finite-difference time-domain simulations is in progress and will be reported in the future.

IV. Correlation Analysis of Biological Cell Spectra

Correlation analysis is a widely used technique in biochemical experiments to recognize specific chemical

components [8] and will be applied here to cell differentiation.

The spectral data were prepared for correlation computations using the following steps. (1) A portion of each spectrum corresponding to a single free spectral range of the cavity was selected. Typically this was the central, highest intensity portion of the spectra. (2) The fundamental mode peak, taken to be the broad, lowest wavelength peak, was assigned a relative wavelength offset of 0 nm. (3) The wavelength offset range was normalized to place the dominate peak of each spectra at the same point. (4) A Lorentzian lineshape curve was fit to the fundamental mode and subtracted from the spectrum thus removing the fundamental which was taken to contain no cell specific information. (5) Lastly, the root-mean-square amplitude of the net spectrum containing the transverse mode transmission peaks was normalized to unity. The resulting spectra for one red blood cell and one white blood cell are shown in Fig. 6 as examples.

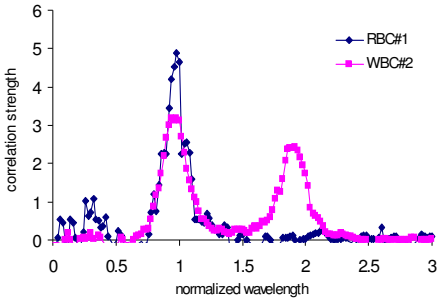

Figure 6. Spectra of a red blood cell and a white blood cell processed according to the steps discussed in the text and ready for a correlation integral.

The correlation coefficients between four red blood cells, two white blood cells, and three yeast cells were then computed and recorded in Table I. The correlation data shows that the two types of blood cells can be differentiated, but that the method is not sufficient to differentiate red blood cells from yeast cells. Additional measurements and analysis are in progress and will be reported.

TABLE I. CORRELATION COEFFICIENT OF SPECTRA FOR RED BLOOD (RBC), WHITE BLOOD (WBC), AND YEAST (Y) CELLS

	RBC1	**RBC2**	**RBC3**	**RBC4**	**WBC1**	**WBC2**	**Y1**	**Y2**	**Y3**
RBC1	1	0.84	0.84	0.872	0.702	0.672	0.843	0.862	0.799
RBC2	0.84	1	0.901	0.847	0.757	0.744	0.820	0.812	0.867
RBC3	0.872	0.901	1	0.878	0.703	0.724	0.681	0.766	0.731
RBC4	0.925	0.847	0.878	1	0.759	0.722	0.907	0.923	0.892
WBC1	0.702	0.757	0.703	0.759	1	0.651	0.691	0.769	0.753
WBC2	0.672	0.744	0.724	0.722	0.651	1	0.571	0.639	0.747
Y1	0.843	0.820	0.681	0.907	0.691	0.571	1	0.970	0.872
Y2	0.862	0.812	0.766	0.923	0.769	0.639	0.970	1	0.925
Y3	0.799	0.867	0.731	0.891	0.753	0.747	0.871	0.925	1

ACKNOWLEDGMENT

This project was supported in part by DARPA under research contract # E-21-F89-G1. The authors thank Dr. S. A. Feld for technical assistance with fabrication.

REFERENCES

[1] J. Emmelkamp, F. Wolbers, H. Andersson, R. S. DaCosta, B. C. Wilson, I. Vermes, and A. V. D. Berg, "The potential of auto fluorescence for the detection of single living cells for label-free cell sorting in microfluidic systems", Electrophoresis, vol. 25, pp. 3740-36735, 2004.

[2] A. C. Romano, E. M. Espana, S. H. Yoo, M. T. Budak, J. M. Wolosin, and S. C. G. Tseng, "Different cell sizes in human limbal and central corneal basal epithelia measured by confocal microscopy and flow cytometry", *Investigative Ophthalmology & Visual Science*, vol. 44, no. 12, pp. 5125-5129, 2003.

[3] C. G. Xie and Y. Q. Li, "Confocal micro-Raman spectroscopy of single biological cells using optical trapping and shifted excitation difference techniques", *J. of Appl. Phys*., 93 (5), pp. 2982, 2003.

[4] P. B. Tarsa, A. D. Wist, P. Rabinowitz, and K. K. Lehmann, "Single-cell detection by cavity ring-down spectroscopy", *App. Phys. Lett.*, vol. 85, no. 19, pp. 4523-4525, 2004.

[5] P. L. Gourley, "Biocavity laser for high-speed cell and tumor biology", *J. of Appl. Phys. D*, vol. 36, no.14, pp. R228-239, 2003.

[6] H. Shao, D. Kumar, S. A. Feld, and K. L. Lear, "Fabrication of a Fabry-Perot cavity in a microfluidic channel using thermocompressive gold bonding of glass substrates", *J. of Microelectro-mechanical Systems*, vol. 14, no. 4, pp. 756-762, 2005.

[7] K. E. Meissner and P. L. Gourley, "Intracavity spectroscopy in vertical cavity surface-emitting lasers for micro-optical-mechanical systems", *Appl. Phys. Lett*., vol. 69, no. 11, pp. 1517-1519, 1995.

[8] E. Gratton, S. Breusegem, N. Barry, Q. Ruan, and J. Eid, "Fluctuation correlation spectroscopy in cells: determination of molecular aggregation", *Biophotonics-Optical Science and Engineering for the 21st Century*, 2004.